Bending Actuation of Hydrogels through Rotation of Light-Driven Molecular Motors

Alexis Perrot, Wen-zhi Wang, Eric Buhler, Emilie Moulin, Nicolas Giuseppone

Hydrogels

How to cite:
International Edition: doi.org/10.1002/anie.202300263
German Edition: doi.org/10.1002/ange.202300263

Bending Actuation of Hydrogels through Rotation of Light-Driven Molecular Motors

Alexis Perrot[+], *Wen-zhi Wang*[+], *Eric Buhler, Emilie Moulin, and Nicolas Giuseppone**

Abstract: The unidirectional rotation of chemically crosslinked light-driven molecular motors is shown to progressively shift the swelling equilibrium of hydrogels. The concentration of molecular motors and the initial strand density of the polymer network are key parameters to modulate the macroscopic contraction of the material, and both parameters can be tuned using polymer chains of different molecular weights. These findings led to the design of optimized hydrogels revealing a half-time contraction of approximately 5 min. Furthermore, under inhomogeneous stimulation, the local contraction event was exploited to design useful bending actuators with an energy output 400 times higher than for previously reported self-assembled systems involving rotary motors. In the present configuration, we measure that a single molecular motor can lift up loads of 200 times its own molecular weight.

Introduction

Molecular machines are nanoscale objects functioning in a Brownian environment and able to convert a source of energy into controlled motion to perform a task.[1–7] They can involve two distinct types of actuating components, i.e. molecular switches or molecular motors.[8–11] With molecular switches, the energy input shifts the equilibrium state of the system, either to reach a new thermodynamic minimum or a metastable state of higher energy. Therefore, molecular switches have the potential to influence their surrounding as a function of their state. In general, the reinitialization of the switch during the backward process cancels any work that was performed during the forward process.[12–14] With molecular motors, however, the absorption of energy leads to an unidirectional and sequence of states which can be repeated autonomously in a cyclic manner. Therefore, molecular motors have the potential to influence their surrounding as a function of the spatial trajectory of their motion and they can produce an increasing mechanical work on their environment upon constant energy supply.[15–18] This is why the continuous and cumulative energy output produced by molecular motors can in principle drive the systems to which they are connected far from their thermodynamic equilibrium.[19–22] This peculiar energetic mechanism rules the functioning principles of many essential biomolecular machines found in living systems, such as ATP-synthase, kinesins, or myosins.[20,21] Similar thermodynamic principles have been also recently exploited by synthetic chemists for the development of a series of innovative artificial molecular motors capable of using various sources of energy, and of producing specific tasks.[22–32] Among them, light-driven rotary motors[18,33–36] introduced by the pioneering work of Ben Feringa and his co-workers[37] are of particular interest because (*i*) their structure is made of a very small number of atoms; (*ii*) they use light as a source of energy, which can be controlled both temporally and spatially, and which does not generate waste; (*iii*) they can reach high functioning frequencies under appropriate conditions;[38,39] and (*iv*) they can deliver high work and force.[40–42] In the present study, we focus on second generation light-driven rotary motors,[43] in which alternating photoisomerization and thermal helix inversion steps lead to the continuous and unidirectional rotation of their rotor part around the double bond and relative to their stator part (Figure 1, with rotor in blue and stator in red).[44]

Light-driven rotary motors have been incorporated in various materials to confer them stimuli-responsive properties.[8,45–48] In particular, they have been used in soft matrices, such as dopants in liquid crystalline systems[49–51] or self-assembled structures,[40,52,53] where changes in configuration and/or conformation of the molecule during its operation led to macroscopic changes of the materials properties. We have also reported their use as mechanically active covalent crosslinks in polymer gels. Investigations on these systems demonstrated that the repetitive unidirectional rotation of the motor under UV light can twist pairs

[*] Dr. A. Perrot,[+] Dr. W.-z. Wang,[+] Dr. E. Moulin, Prof. Dr. N. Giuseppone
SAMS Research Group, Université de Strasbourg, CNRS, Institut Charles Sadron UPR 22
67000 Strasbourg (France)
E-mail: giuseppone@unistra.fr

Prof. Dr. E. Buhler
Matière et Systèmes Complexes (MSC), UMR CNRS 7057, Université Paris Cité
Bâtiment Condorcet, 75013 Paris (France)

Dr. A. Perrot[+]
School of Chemistry, University of Birmingham
Birmingham, B15 2TT (UK)

[+] These authors contributed equally to this work.

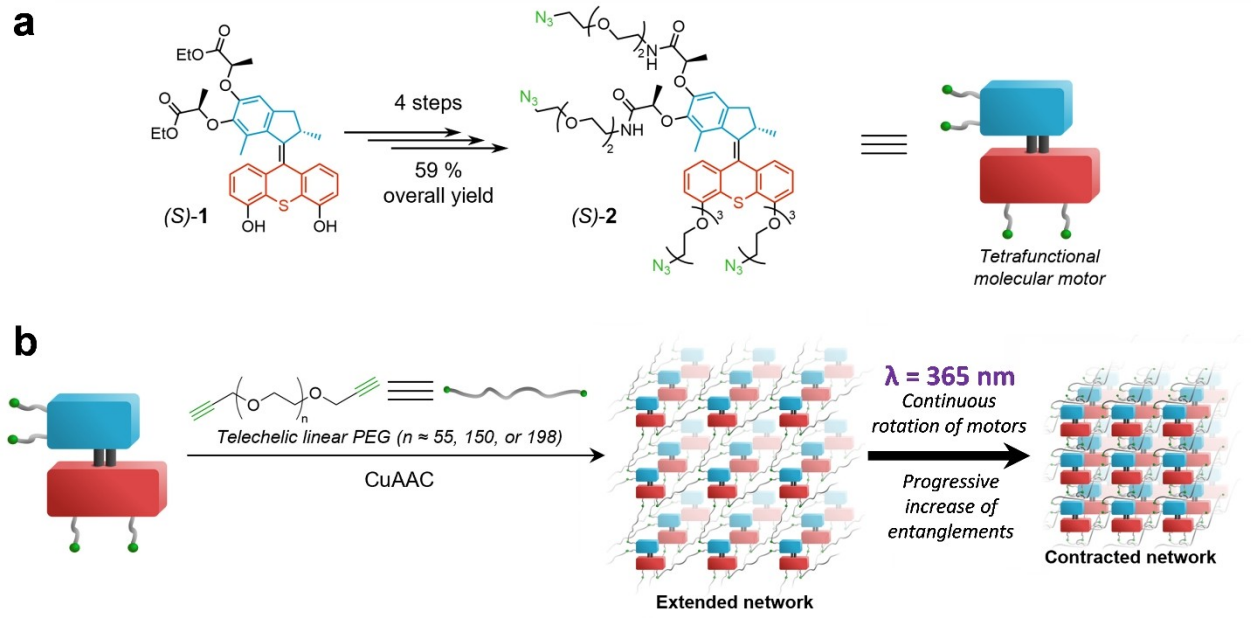

Figure 1. **a)** Structure and representation of tetra-azide motor (*S*)-**2** used as a tetrafunctional crosslinker. The 'stator' is represented in red and the 'rotor' in blue. **b)** Reticulation of telechelic bis-alkyne PEG with tetrafunctional crosslinkers resulting in the formation of a photoactive gel. Irradiation of the material with UV light triggers the unidirectional rotation of the motors, thereby creating new physical entanglements, and leading to the macroscopic contraction of the network and syneresis.

of polymer chains into the network. The creation of these new entanglements effectively changes the swelling equilibrium of the gels, which macroscopically contract over time under light irradiation.[45] Our initial studies mainly focused on the impact of the motor on the mechanical and structural properties of the gels swollen in organic solvents.[54,55] In the present work, we now shift our focus on the polymer network itself, and we elucidate key internal and external parameters affecting the operation of these machines in soft materials. By doing so, we reveal important improvements which include: (*i*) the efficient functioning of these gels in water, a solvent of interest for new potential applications, (*ii*) the improvement of their kinetic contraction efficiency by one order of magnitude, and (*iii*) their implementation as macroscopic actuators in which a single molecular motor can lift up to 200 times its own molecular weight.

Results and Discussion

Modular Synthesis of Polymer Networks

Previously reported light-sensitive contractile polymer gels were formed by reticulating molecular motors bearing two orthogonally functionalized polymer chains upon copper-catalyzed azide-alkyne cycloaddition (CuAAC).[45,54] However, this design requests to synthesize, for each particular gel, a particular polymer-motor conjugate before reticulation. Hereafter, all the chemical gels are based on a new design in which tetrafunctional motors are used as crosslinking agents for telechelic macromolecules. In this topology, linear bis-alkyne polymers are crosslinked by a tetra-azide light-sensitive molecular motor (Figure 1a). Advantageously, this methodology allows that a unique molecular motor can reticulate polymer chains with different molecular weights, topologies, and/or chemical structures, and that other functional crosslinking units can be easily added to the formulation. The active tetra-functional motorized units were obtained by grafting short triethylene glycol (TEG) spacers to a generic second-generation molecular motor.[45,56] Two types of TEG spacers with terminal azides were synthesized: the first one bearing a *p*-toluene sulfonate end group for functionalization of the stator part, and the second one bearing an amino end group for functionalization of the rotor part.

Starting from the partially deprotected molecular motor *(S)*-**1**, whose gram-scale synthesis was previously reported,[56] we obtained tetra-azide motor *(S)*-**2** after three steps consisting in an alkylation, a saponification and an amidation with an overall yield of 59 % (see Supporting Information for the synthetic protocols and characterizations of products). Then, alkyne-terminated poly(ethylene glycol) (PEG) chains of variable molecular weights were synthesized from commercially available telechelic α,ω-dihydroxy-PEG. Deprotonation of the terminal alcohols with sodium hydride and subsequent nucleophilic substitution on propargyl bromide led to α,ω-dipropargyl-PEG with average molecular weights $M_W \approx 2400$, 6700 and 8700 g mol^{-1}, which we refer to as $\mathbf{PEG_{2400}}$, $\mathbf{PEG_{6700}}$ and $\mathbf{PEG_{8700}}$, respectively (see Supporting Information).

In a previous study, we showed that an optimal mechanical and structural response of these gels is achieved

when they are chemically reticulated at the overlap or crossover concentration c* separating dilute and semidilute regimes where chains are entangled and form a network.[54,55] Such concentration ensures quantitative crosslinking, while minimizing the amount of initial entanglements that could impair the contraction of the network under UV light. Incidentally, the overlap concentration also determines the concentration of motors needed for the preparation of the gels in stoichiometric proportions between azide and alkyne groups. Therefore, we determined at this stage the overlap concentration of the free telechelic PEG chains in different solvents using intrinsic viscosity [η] measurement of the solution (see Table 1). We subsequently prepared a series of gels at c* using different solvents to achieve crosslinking (entries **Gel$_1$** and **Gel$_2$**), or with different thicknesses (entries **Gel$_2$**-**Gel$_5$**) and different molecular weights (entries **Gel$_2$**, **Gel$_6$** and **Gel$_7$**) (Table 1, see Supporting Information for details on the preparation). Several parameters were then investigated to better understand and optimize the contraction behavior of these materials.

Optimization of the Contractile Behavior of Gels Cross-linked with Light-Driven Molecular Motors

The local structural changes under contraction of such gels at c* were investigated using small-angle neutron scattering (SANS),[57] a technique much more sensitive to the PEG chains (see Supporting Information for details concerning the contrasts). We retrieve the typical overall behavior of cross-linked networks swollen in good solvent with the following sequence (Figure 2a and Supporting Information for other gels): (*i*) the signal of excluded volume chains at high q, where q is the scattering vector, with a characteristic $q^{-5/3}$–q^{-1} transition at the length scale of the PEG chain persistence length ($\approx$1 nm in average); (*ii*) a Lorentzian variation associated with the correlation length ξ of the entangled network at mid-q; (*iii*) and finally a low-q upturn showing the presence of heterogeneities larger than the SANS length scale, a general characteristic of gels.

To track the macroscopic gel contraction, a piece of gel of $\approx$0.25 cm^2 swollen in an appropriate solvent was immersed in a cylindric cell, which was then placed in between a camera and a UV light source. The camera captured the evolution of the surface over irradiation time, which can be converted into an evolution of the relative volume by considering an isotropic 3D contraction (see Supporting Information for experimental details).

Table 1: List of prepared PEG gels crosslinked with molecular motor *(S)*-**2**.

Entry	Reticulation solvent	Thickness [mm]	M_w [g mol^{-1}]	c* [mg mL^{-1}]	[η] = 1/c* [cm^3 mg^{-1}]
Gel$_1$	CH_2Cl_2	0.5	6700	52	0.0193
Gel$_2$	DMF	0.5	6700	68	0.0148
Gel$_3$	DMF	0.75	6700	68	0.0148
Gel$_4$	DMF	1	6700	68	0.0148
Gel$_5$	DMF	1	6700	68	0.0148
Gel$_6$	DMF	0.5	2400	88	0.0113
Gel$_7$	DMF	0.5	8700	58	0.0171

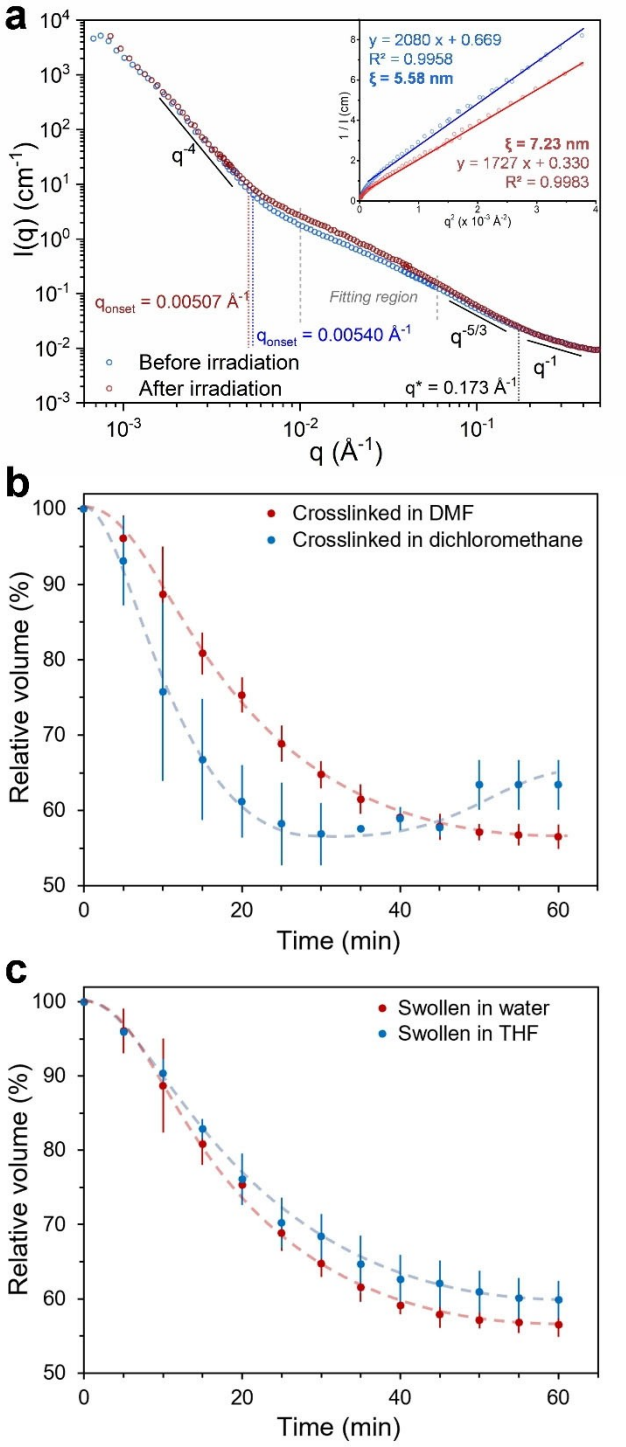

Figure 2. **a)** SANS scattering profiles obtained before light irradiation (blue dots) and after 40 min of irradiation (red dots) for **Gel$_4$** at c* = 68 mg cm^{-3}. Details concerning the fit of the data are given in the Supporting Information; **b)** Contraction of **Gel$_1$** (blue) and **Gel$_2$** (red), swollen in water, under UV light at 365 nm (80 mW cm^{-2}); **c)** Contraction of **Gel$_2$**, swollen in water (red) or THF (blue), under UV light at 365 nm (80 mW cm^{-2}). Error bars represent the standard deviation over at least two samples. Dashed lines are guides to the eye.

Solvent quality may significantly alter the contractile behavior of these mechanically active gels because it regulates the chains interaction and conformation. First, the reticulation solvent—in which the copper-catalyzed azide-alkyne cycloaddition is achieved—influences the initial structure of the network. Here the intrinsic viscosity is scaling with the degree of polymerization like $[\eta] \approx N^{1/2}$ (see Table 1), indicating an ideal chain conformation for the telechelic chains and possibly explaining the formation of heterogeneities. However, the experimental scaling exponent is usually found to be smaller than 4/5 for short chains - as here - in good solvent. Formation of heterogeneities may mostly originate from the specific PEG extremities. Second, the swelling solvent— in which the light-driven contraction takes place—determines the structure of the network and the conformation of the polymer strands as more twists are generated under UV. We compared two crosslinking solvents for the formation of the gels by CuAAC: dimethylformamide (DMF) and dichloromethane (Figure 2b) (see Table S2 for reticulation conditions). The contraction in water of **Gel$_1$**, formed in dichloromethane, is faster than the one of **Gel$_2$**, formed in DMF, and although they both reach the same minimal relative volume of ≈55 %. The formation of new entanglements, leaving more space between newly twisted pairs, is accompanied by a significant increase of the gel correlation length, which is related to the mesh size of the network. This increase was found to be maximal at c* and strongly correlated with the contraction efficiency.[55] Figures S9 also display such behavior with a significant mesh size variation for irradiated gels reticulated both in CH_2Cl_2 or DMF and swollen at c*. Importantly, such a variation is not observed for control gels with non-rotative episulfide motors and no contractile behavior (see Figure S9.d). We found $\Delta\xi \approx 6.8$ nm for a gel similar to **Gel$_1$** at c* (see Figure S9.b), showing a strong contraction efficiency. However, **Gel 1** slightly degrades over time as seen by its loss of fluorescence and by an increase in relative volume at the late stages of irradiation. Therefore, considering that degradation occurs, we favored the formation of gels in DMF for the following study related to the influence of the swelling solvent. Water and THF are both good solvents for PEG as inferred from SANS displaying the characteristic signature for the size of excluded volume network strands: $R \approx N^{3/5}$ (i.e., the $q^{-5/3}$ power law). They were thus compared as swelling solvents to elucidate their impact on the kinetics of contraction (Figure 2c). The two solvents gave statistically identical results, both in terms of kinetics and of minimal relative volume, indicating that the chemical nature of the solvent has little influence on the contraction, provided it is a good solvent for the polymer strands. While a thickness of 2 mm was used for SANS, a significant $\Delta\xi$ is observed in all cases at c* (see Supporting Information). Obviously, the possibility to actuate hydrogels is an important and attractive novelty of potential applicative interest, and we kept water as the swelling solvent for the entire following study.

Pieces of gels were formed in molds of defined thicknesses (comprised between 0.5 and 2 mm) to study the influence of this parameter on the contraction (Figure 3). In terms of kinetics, the thinner gels contract faster, a phenomenon that can be attributed to the penetration depth of UV light inside the material. Indeed, for thicker samples, motors away from the light source receive less light and hence rotate slower, and consequently the average rotation speed of the motors and the contraction speed of the whole material are lower. These results also show that for thicker gels the contraction is not isotropic anymore, and this aspect will be implemented for the design of actuators in the last part of this article. When looking at the final contraction values, the thinnest gels **Gel$_2$** and **Gel$_3$** reach the same relative volume, indicating that this parameter is mainly related to the structure of the network. However, **Gel$_4$** and **Gel$_5$** do not reach this value because only the side of the gel closest to the light source contracts efficiently.

By varying the light intensity from 7 mW cm^{-2} to 368 mW cm^{-2}, **Gel$_2$** shows faster contraction for higher irradiation powers, until this speed reaches a plateau above 80 mW cm^{-2} (Figure 4a–c). In the literature, kinetic models established by Feringa and co-workers relate the irradiation

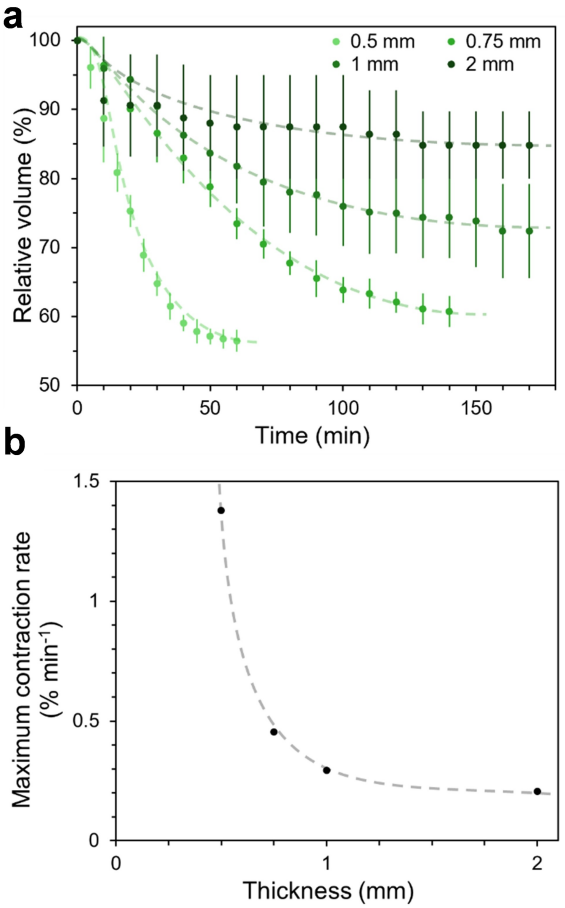

Figure 3. **a)** Contraction of **Gel$_2$**, **Gel$_3$**, **Gel$_4$**, and **Gel$_5$**, with thicknesses of 0.5, 0.75, 1, and 2 mm respectively, under UV light at 365 nm (80 mW cm^{-2}); **b)** Maximum contraction rate of PEG gels as a function of their thickness. Gels were crosslinked in DMF and swollen in water. Error bars are standard deviation over at least two samples. Dashed lines are guides to the eye.

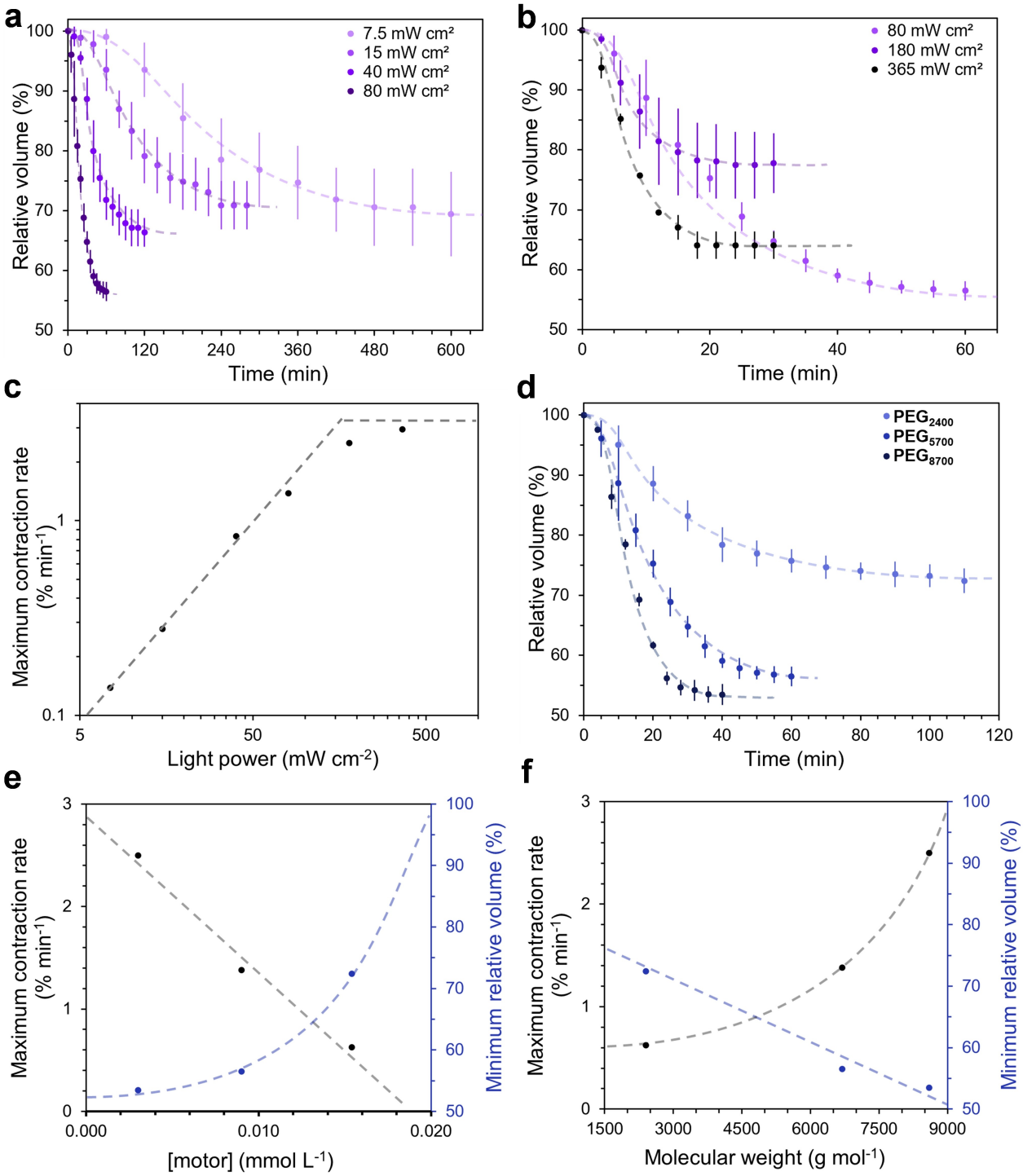

Figure 4. **a–b)** Contraction of **Gel_2** under UV light at 365 nm, at **a)** low light power (7.5, 15, 40 and 80 mW cm^{-2}) and **b)** high light power (80, 180 and 365 mW cm^{-2}); **c)** Maximum contraction rate for **Gel_2** as a function of light power; **d)** Contraction of **Gel_2** (PEG_{2400}), **Gel_6** (PEG_{5700}), and **Gel_7** (PEG_{8700}) under UV light at 365 nm, 80 mW cm^{-2}; **e)** Maximum contraction rate as a function of the concentration of molecular motors inside the gels; **f)** Maximum contraction rate as a function of the molecular weight of PEG used to form the gels. The gels were formed in DMF and swollen in water. Error bars represent the standard deviation over at least two samples. Dashed lines are guides to the eye.

power to the rotation frequency of molecular motors in solution.[58] It was demonstrated that higher light intensities lead to faster rotation rates of individual molecular motors in solution until a limiting regime is reached for high photon densities, and at which the system becomes thermally rate limited. Here, the plateau reported in Figure 4c seems in agreement with this kinetic model extended to the macroscopic output of our system, even if we know that the

frequencies reached in the chemical gel are much lower than those observed for free motors in solution.[45] However, further studies of these gels over a large range of temperatures proved to be very difficult in water due to their volume variation caused by temperature itself.[59,60] It remains therefore difficult to decipher the photochemical and thermal contributions leading to the contraction with a sufficient precision.

In addition, for light powers below 80 mW cm^{-2}, the average final contraction volume decreases with increasing light power, from 69±7% at 7 mW cm^{-2} to 58±2% at 80 mW cm^{-2} (Figure 4a). This trend suggests that molecular motors can create more entanglements with higher light intensities, and consequently further shift the swelling equilibrium to smaller relative volumes. This is coherent with the fact that the final swelling equilibrium of these gels occurs when the work of the photoactive crosslinks is counterbalanced by the mechanical strain generated in the entangled network, as recently demonstrated for individual rotary motors.[41] However, above 80 mW cm^{-2}, this trend does not hold (Figure 4b), probably due to some photochemical degradation occurring under stronger UV light. While this effect should not significantly alter the maximum contraction rates (measured in the first minutes of contraction), it considerably limits the accuracy and reproducibility of the final contraction volumes. Therefore, the following study on the influence of the molecular weight of the polymer was performed at the optimal value of 80 mW cm^{-2}.

As explained above, we formed a series of PEG gels with PEG chains of different molecular weights at their respective c*. Very interestingly, we found that gels formed from longer polymer chains contract faster and reach lower relative volumes (Figure 4d–f). Concomitantly, a lower variation of the gel correlation length is observed for short PEG 3000 chains (see Supporting Information). One key parameter of the gels modified by using polymer chains of different molecular weights is the initial strand density $\Phi_{s,i}$ (parts of chain between efficient motors and/or entanglements in the network). Considering that the gels are formed at their respective c*, $\Phi_{s,i}$ is defined as:

$$\Phi_{s,i}=c^* \times \nu \quad (1)$$

where ν is the specific volume of the monomer. Since $c^* \approx N^{-4/5}$ in good solvent, $\Phi_{s,i}$ is lower for gels formed from longer PEG chains and individual strands can move more freely. The energy barrier for molecular motors to twist them together is then lower, thereby leading to faster kinetics (Figure 4f). As $\xi \approx \varphi^{-3/4}$ for semi-dilute solutions in good solvent, the correlation length of the network is also higher. While it could be affected by the distribution of heterogeneities, ξ is effectively higher for larger M_W as compared to PEG 3000 (see Supporting Information).

Another parameter affecting the rotation kinetics of molecular motors is their concentration in solution.[58] Lowering the concentration of molecular motors in the gels essentially means that there are more photons available per motor for their rotation, and, hence, that they rotate faster and lead to faster contraction kinetics (Figure 4e). Overall, we suggest that the contraction rate results from a combination of the impact of the strand density and concentration of molecular motors in the gel. In addition, because longer polymer chains have lower c*, the initial number of crosslinks is lower in the gel. Therefore, more new entanglements can be created by the rotation of molecular motors before reaching a concentration of (chemical and physical) crosslinks that leads to a loading energy in the network sufficient to counteract the torque of the molecular motors.[41] In other words, we suggest that when gels are formed from PEG with higher molecular weights, the active crosslinks will create a higher number of twisted entanglements and, hence, will further shift the swelling equilibrium towards lower relative volumes (Figure 4f).

From these series of investigations, it appears that the best contraction speed should be achieved by irradiating thinner gels crosslinked using longer polymer chains at c* and irradiated at higher light power. Therefore, we determined the performance of such an 'optimized' **Gel$_7$** formed with **PEG$_{8700}$**, having a thickness of 0.5 mm, and irradiated with a UV light intensity of 365 mW cm^{-2} (Figure 5 and supplementary movie 1). This material shows a maximum contraction rate of approximately 5% min^{-1}, and a contraction half-time $t_{1/2}$ of ≈5 min. Compared to our initial reports,[45] it corresponds to a 10 times faster contraction.

Macroscopic Bending Actuation of Hydrogels Cross-linked with Molecular Motors

As described above, we hypothesized that the relatively low contractile efficiency of **Gel$_5$**, with a thickness of 2 mm, was caused by the limited light penetration throughout the material and, hence, the differential stimulation of the motors in the network (see above and Figure 3). While this phenomenon should be avoided for the bulk contraction of gels, it becomes desirable to design bending actuators,

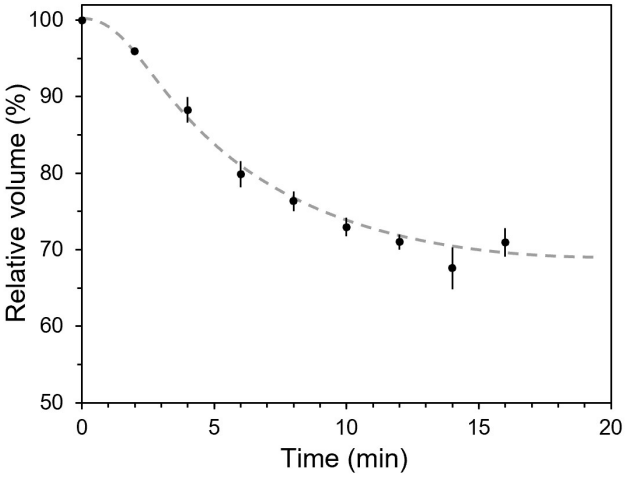

Figure 5. Contraction of **Gel$_7$** under UV light at 365 nm and at 365 mW cm^{-2}. Error bars represent the standard deviation over two samples. The dashed line is a guide to the eye.

whose directional deformation should result from the asymmetric change of volume along the thickness of the material. Therefore, thin strips of **Gel$_5$**, with a length of 1.5 cm and a width of 0.5 cm, suspended in degassed and deionized water, were irradiated with UV light of appropriate intensity to trigger their bending motion, which we quantified by measuring their bending angle θ over time (Figure 6 and supplementary movie 2).

By neglecting the deformation along the width and the thickness of the material (considering their lower dimensions compared to the length of the strips), a simplistic model relating the linear deformation of the material along the length of the irradiated face λ and the bending angle θ can be written (see Supporting Information for details):

$$\lambda = 1 - \theta\frac{d}{L} \qquad (2)$$

with d and L the thickness and the length of the gel, respectively, and θ expressed in radians.

Importantly, the determination of λ^3 allows for a direct comparison between the bending behavior of **Gel$_5$** and the bulk contraction of thin gels described in the previous paragraphs, because it gives the relative volume resulting from an isotropic deformation when all three dimensions are contracted by λ.

We limited our investigations to intensities lower than 20 mW cm^{-2}, where less than half of the thickness of the gel is stimulated, as indicated by its fluorescence. Although this maximum power is not optimal for the actuation speed, we know however that a maximum deformation should be reached over sufficient time (see above).

Similarly to the contraction speed of **Gel$_2$** (Figure 4), the strips of **Gel$_5$** bend faster when irradiated with light of higher intensities (Figure 6b). Over the range of light power tested, the maximum bending rates ranged between 0.06 and 1° min^{-1}. When converted to the corresponding contraction rates λ^3 (Figure 6c), the maximum rate of local volume change of the irradiated face of the strips ranged between 0.033 and 0.56 % min^{-1}. These values were compared to the experimental trend determined for **Gel$_2$** formed from PEG chains of the same molecular weight but with a thin thickness (see above and Figure 6d). The same linear correlation between the contraction rate and the light power is apparent, consistent with our results for thin gels. Remarkably, the experimental rates measured for **Gel$_5$** are also in the same order of magnitude as the ones measured for **Gel$_2$**. The slight increase in contraction rate observed for **Gel$_5$** may be explained by the fact that the motors close to the surface, responsible for the bending behavior, rotate slightly faster than the motors in the bulk of **Gel$_2$** because of the limited light penetration. Nevertheless, these results demonstrate that the asymmetric contraction of thick self-standing gels is similar to the bulk contraction of thin gels and shows the validity of our model for estimating the maximum bending rate.

For light intensities between 6.5 and 20 mW cm^{-2}, all gels reach a similar final bending angle of approximately 50°. However, at a very low light power of 1.6 mW cm^{-2}, the

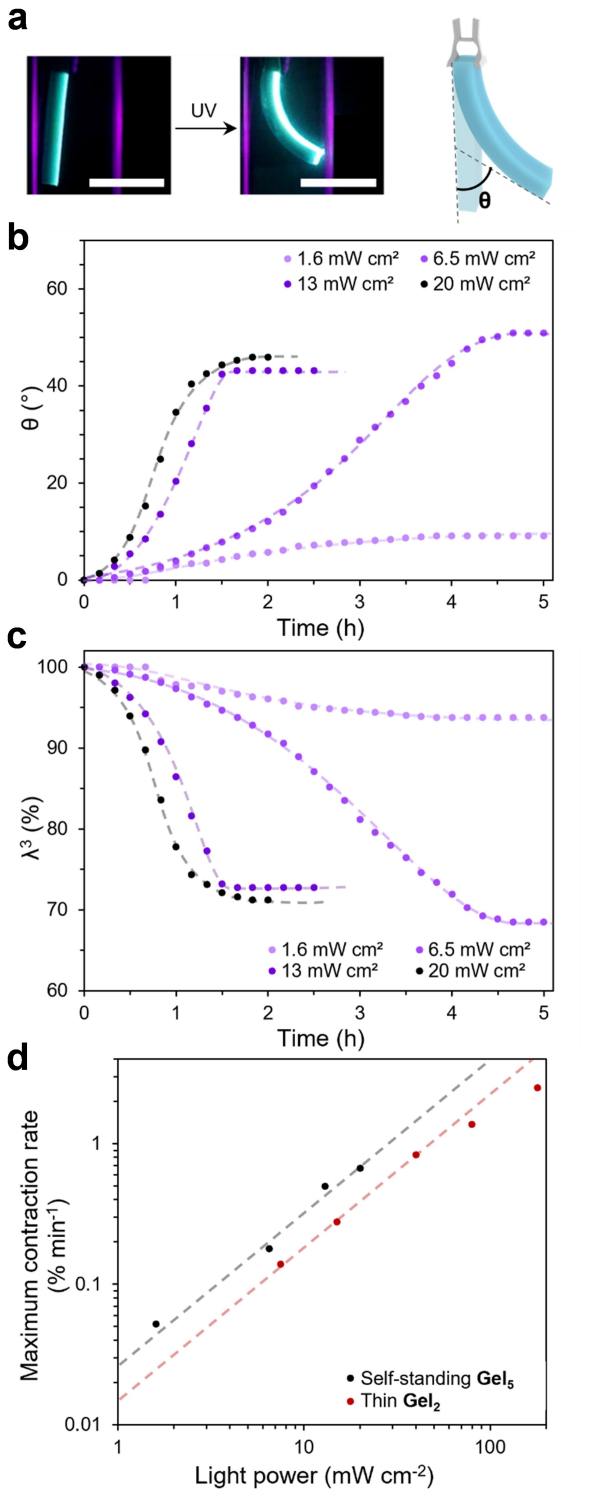

Figure 6. **a)** *Left*, snapshots of the bending motion of strips of **Gel$_5$** under UV light; *right*, schematic representation of the gel with its bending angle θ. Scale bars: 1 cm; **b)** Bending angle θ of thin strips of **Gel$_5$** as a function of irradiation time for different light intensities (365 nm), and **c)** corresponding relative contraction λ^3. Gel dimensions: 15×5×2 mm^3; **d)** Comparison between the maximum contraction rate of strips of **Gel$_5$** (black dots) anf of bulk **Gel$_2$** (thickness: 0.5 nm, red dots) at different light powers. Dashed lines are guides to the eye.

system barely bends over the time of the experiment (Figure 6b). Except for this case, when converted into λ^3, the bending angle corresponds to approximately 65–70 % of the initial volume, which is identical to the values obtained for thin **Gel$_2$** in that intensity range (Figure 4). These results show that the extent of the contraction is not altered when irradiating self-standing gels and, similarly to the bending rate (see above), the bending angle can be predicted from the contractile behavior of the corresponding thin gels. Our subsequent experiments were conducted with UV light at 6.5 mW cm^{-2}, as it gave slightly higher final bending angles and the gels showed less degradation over time at that power.

The linear deformation λ determined by our model is, in fact, related to the difference of deformation between the irradiated and non-irradiated surfaces (see Supporting Information). Consequently, irradiation of one side of the strip followed by irradiation of its other side, should lead to a back and forth bending of **Gel$_5$** because of the final identical deformation of both surfaces of the strip. We confirmed that behavior experimentally (Figure 7a–b, and supplementary movie 3). Importantly, the bent gels could sustain their shape for weeks in the dark, highlighting the mechanical stability of our self-standing networks, and the non-reversible rotation of the motor in these conditions.[41] However, since the actuation is caused by asymmetric deformation of the material, the gel can be straightened by irradiating the other face of the strip until the contraction is homogeneous along its width. It should be noted that the bending/contraction rates is slightly slower when coming back after a first actuation, which can be explained by a higher tension of the chains in the already contracted part of the network, thus decreasing the motor frequency.

Further, since λ is an apparent linear deformation resulting from the difference of deformations between both sides, it should be possible to achieve specific bending angles with a dual and simultaneous irradiation of each side using different light intensities. We tested this hypothesis by

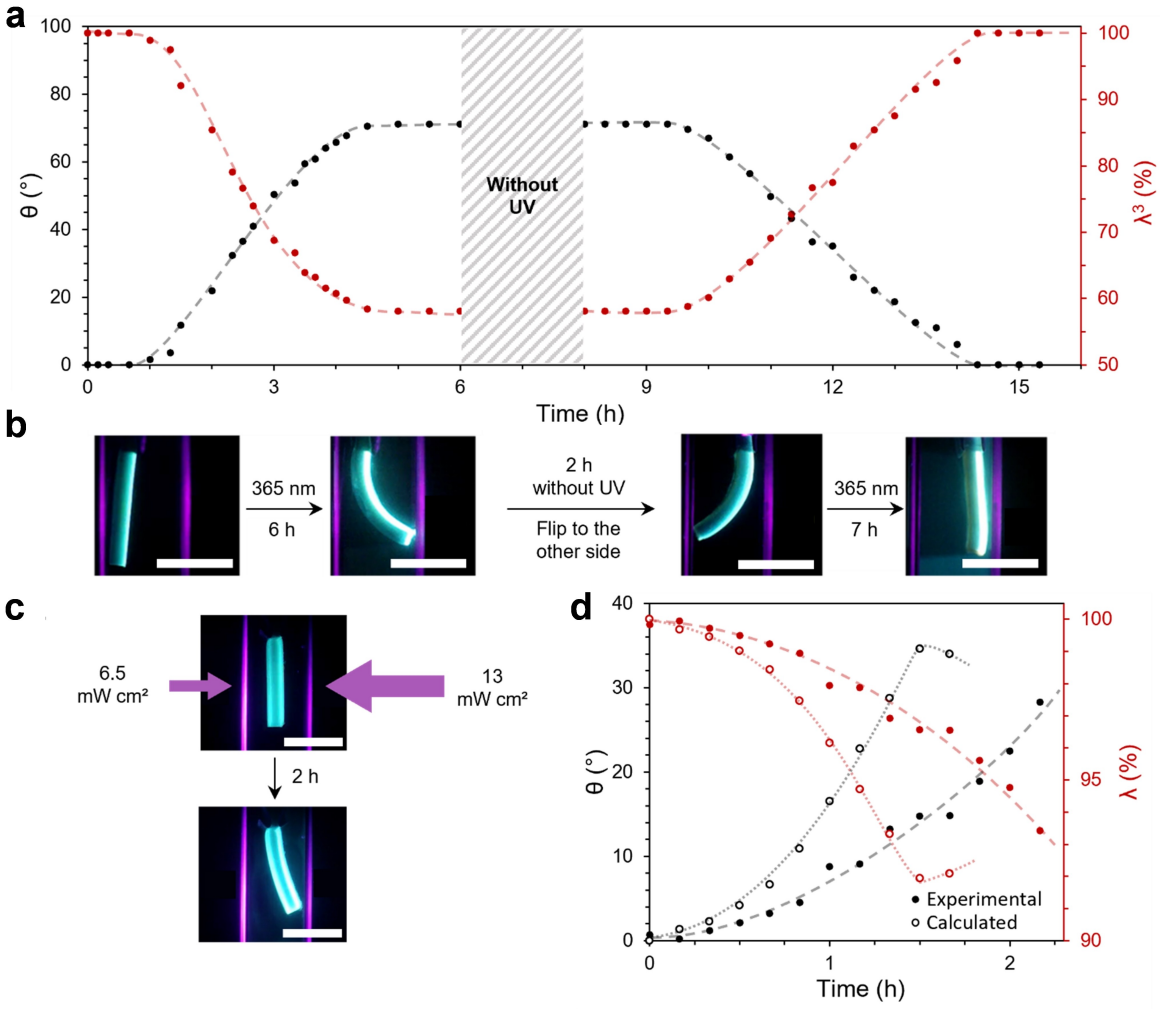

Figure 7. **a)** Back-and-forth bending of a strip of **Gel$_5$** under successive irradiation of each sides of the strip, and **b)** corresponding snapshots of the gel. The gel was irradiated with UV light at 365 nm and 6.5 mW cm^{-2} power intensity; **c)** Snapshots of simultaneous dual-side irradiation (365 nm) of a strip of **Gel$_5$** and **d)** corresponding calculated (open circles) and experimental (closed circles) bending angle (black) and linear deformation (red) over time. Scale bars: 1 cm. Dashed lines are guides to the eye.

irradiating a strip of **Gel$_5$** with UV light at 6.5 mW cm^{-2} on one side, and 13 mW cm^{-2} on the other (Figure 7c–d), and compared the experimental bending behavior to the calculated one determined from the difference of linear deformations at different light intensities, which was measured beforehand (Figure 6c). Comparison between the experimental and the calculated values indicates again that our simple model gives reasonable estimates of the bending behavior: the time at which the maximum bending angle is reached was calculated to be 1.5 h, and was experimentally 2.2 h. Moreover, a maximal bending angle of 35° was calculated, which is reasonably close to the experimental value of 28°. Therefore, the final bending angle of our contractile gels cannot only be determined by the irradiation time (see above), but also by the simultaneous and continuous asymmetric irradiation of both sides of the strips with different light intensities. Overall, these results show that a range of bending angles can be achieved and adjusted with proper modes of irradiation power, time, and direction.

Considering equation (2), for the same deformation λ, the bending angle θ should increase with the length of the gel L. Consequently, we compared the bending behavior of two strips of **Gel$_5$** with lengths of 1.2 and 1.5 cm, respectively, while keeping the other dimensions identical (5 × 2 mm^2) (Figure 8a). The strip with the lowest length (1.2 cm) reaches a final bending angle of 50°, while the one with a higher one (1.5 cm) reaches a final bending angle of 60°. Importantly, the linear deformation of the irradiated faces of both strips is almost identical throughout the course of irradiation in both cases, confirming the validity of our model on that aspect. Therefore, the bending behavior of our self-standing gels can also be controlled by the initial shape of our materials.

Finally, we investigated the generation of mechanical work from the deformation of our self-standing strips of **Gel$_5$** to lift different weights. A small hook was pierced through the strips of gels, to which fishing weights of different masses were attached.

First, the final bending angle gradually decreases with increasing masses, from approximately 70° without load to 40° with a load of 43 mg, which represents a decrease of 45 % (Figure 8b). Second, the bending rate also decreases with increasing weights, from approximately 0.53° min^{-1} when there is no load, to approximately 0.21° min^{-1} with a weight of 43 mg, which corresponds to a 61 % decrease (supplementary movie 4). One can reasonably suggest that the stretching of the irradiated face by the load constrains the twisting motion by the motor, and therefore affects both the final bending angle and bending rate at the macroscale.

The heaviest lifting performance was achieved with one strip of **Gel$_5$** bearing a load of 55.5 mg (Figure 8c). The weight was lifted 3.5 mm above its initial position, corresponding to a difference of gravitational potential energy of 2 μJ (see Supporting Information for details). Since the concentration of *(S)*-**2** in **Gel$_5$** is 5.3 mM, the energy generation of our self-standing photoactive networks corresponds to 0.38 mJ L mol^{-1} of molecular motors, or 129 mJ L g^{-1} of photoactive core (rotor and stator only). This value is approximately 400 times higher than the previously

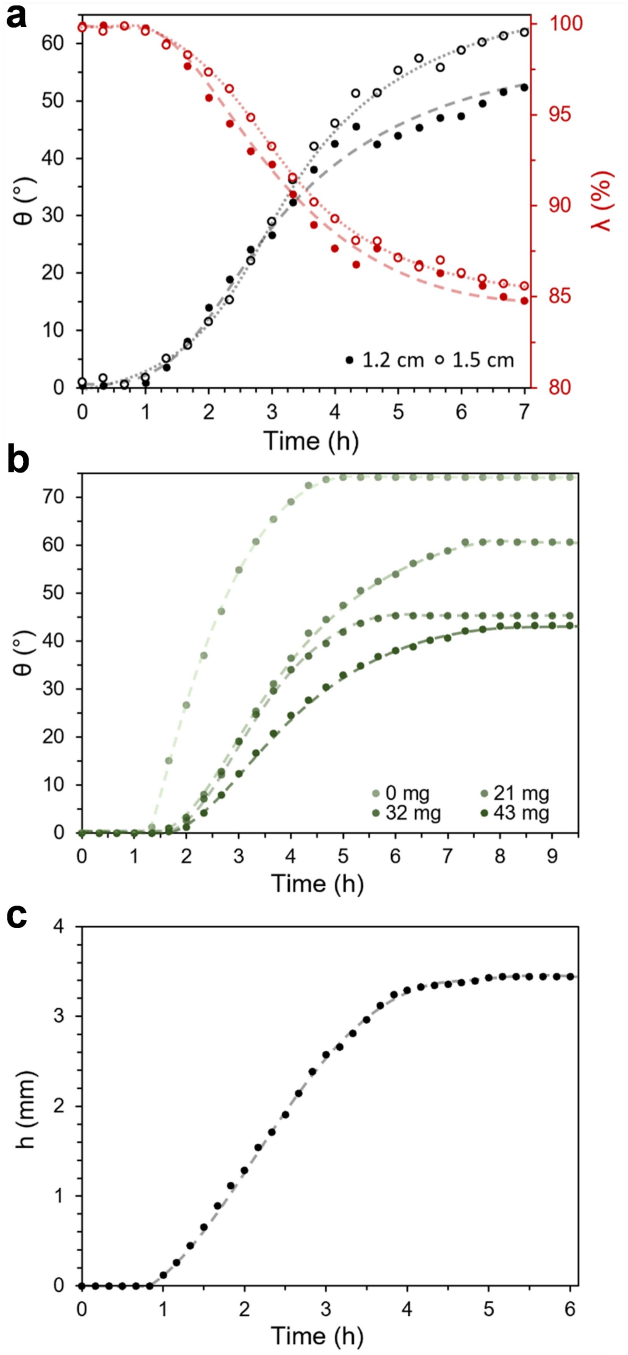

Figure 8. **a)** Comparison of the bending angle (black) and linear deformation (red) of strips of **Gel$_5$** with different lengths (open circles: 1.5 cm; closed circles: 1.2 cm) under UV irradiation (365 nm, 6.5 mW cm^{-2}); **b)** Bending angle of strips of **Gel$_5$** with different weights over time under UV light; **c)** Lifting height of a load of 55.5 mg by a strip of **Gel$_5$** over time under UV light irradiation. UV light: 365 nm, 6.5 mW cm^{-2}. Dashed lines are guides to the eye.

reported reference for actuators using molecular motors as switches into self-assembled supramolecular fibers (1 μJ L mol^{-1} of motors).[40] Considering the dimensions of the strips (15 × 5 × 2 mm^3), **Gel$_5$** contains 0.27 mg of motor core (see Supporting Information for details); therefore, it

can lift approximately 200 times its own weight when integrated in a covalent gel. These performances highlight that the covalent integration of photoactive units in actuators is a promising strategy for the generation of mechanical work at the micro- and macroscopic scales from nanoscopic motion. Importantly, these values are a low estimate of the lifting capacity of that kind of molecular motors in hydrogels, since the bending behavior results from an asymmetric irradiation where only a part of the total amount of motors is used for the actuation, and since a low light power was used because of the relatively small thickness of the materials.

On can finally notice that the magnitude of the flexural deformation depends on the irradiation force, the sample geometry and the bending or flexural modulus, which corresponds to the tendency for a material to resists bending as seen in Figures 6 and 7. The latter is assumed to be equal to the elastic modulus of the gel, which was determined in a previous work using rheological measurements.[54] As only a part of motors is used for the actuation within this asymmetric irradiation, the elastic modulus should be close to the value determined for the extended gel; i.e. 6800 Pa for PEG5000 at c*. This gives a lower bound for the bending modulus. The value determined for the contracted gel, 20500 Pa, gives a higher bound.

Conclusion

Molecular motors have the potential to become the key components of a new generation of smart materials and actuating devices. In order to integrate their individual cyclic trajectories in collective motion, it appears of utmost importance to define how to connect them with one another and with their environment up to the macroscopic scale. In the case of this study involving light-driven rotary molecular motors covalently linked to polymer networks, we have highlighted two key parameters impacting their actuation efficiency as hydrogels: *i*) the photon density available per motor, which drives its forward rotation and shifts the material further from its initial swelling equilibrium, and *ii*) the strand density of the network, which can counteract the forward rotation of the photoactive crosslinks because of the mechanical strain built in the network meshes. Our systematic study led to the preparation of self-standing gels where the operation of molecular motors led to bending actuators revealing an energy output 400 times higher than in the most comparable previously reported systems, and capable to lift 200 times the weight of the molecular motors at the origin of their work. We anticipate that the general principles outlined in this study will be instrumental to further develop efficient materials coupling molecular motors in various soft networks.

Acknowledgements

The authors wish to acknowledge the Ministère de la Recherche et de l'Enseignement Supérieur, and the Chinese Scholarship Council for fellowships to AP and WW, respectively. They also thank the "Jean-Marie Lehn Foundation". They acknowledge the "Plateforme de caractérisation des polymères" from the Institut Charles Sadron for GPC and Dr. Jean-Marc Strub for Maldi experiments. They also wish to thank the Laboratoire Léon Brillouin (LLB-Saclay, France) and the Institut Laue Langevin (ILL-Grenoble, France) for beam-time allocations as well as F. Cousin and S. Prevost for their precious help during the SANS experiments on PAXY and D11, respectively. The authors are grateful to Dr. Pierre Lutz for fruitful discussions.

Conflict of Interest

The authors declare no conflict of interest.

Data Availability Statement

The data that support the findings of this study are available from the corresponding author upon reasonable request.

Keywords: Light-Responsive Materials · Molecular Motors · Polymer Networks · Soft Actuators

[1] E. R. Kay, D. A. Leigh, F. Zerbetto, *Angew. Chem. Int. Ed.* **2007**, *46*, 72–191; *Angew. Chem.* **2007**, *119*, 72–196.
[2] V. Balzani, A. Credi, M. Venturi, *Molecular Devices and Machines*, Wiley-VCH, Weinheim, **2008**.
[3] J.-P. Sauvage, *Angew. Chem. Int. Ed.* **2017**, *56*, 11080–11093; *Angew. Chem.* **2017**, *129*, 11228–11242.
[4] J. F. Stoddart, *Angew. Chem. Int. Ed.* **2017**, *56*, 11094–11125; *Angew. Chem.* **2017**, *129*, 11244–11277.
[5] B. L. Feringa, *Angew. Chem. Int. Ed.* **2017**, *56*, 11060–11078; *Angew. Chem.* **2017**, *129*, 11206–11226.
[6] C. J. Bruns, J. F. Stoddart, *The Nature of the Mechanical Bond*, Wiley, Hoboken, **2016**.
[7] L. Zhang, V. Marcos, D. A. Leigh, *Proc. Natl. Acad. Sci. USA* **2018**, *115*, 9397–9404.
[8] D. Dattler, G. Fuks, J. Heiser, E. Moulin, A. Perrot, X. Yao, N. Giuseppone, *Chem. Rev.* **2020**, *120*, 310–433.
[9] M. Kathan, S. Hecht, in *Out-of-Equilibrium (Supra)Molecular Syst. Mater.*, Wiley, Hoboken, **2021**, pp. 275–304.
[10] S. Corra, M. Curcio, M. Baroncini, S. Silvi, A. Credi, *Adv. Mater.* **2020**, *32*, 1906064.
[11] E. Moulin, L. Faour, C. C. Carmona-Vargas, N. Giuseppone, *Adv. Mater.* **2020**, *32*, 1906036.
[12] J. D. Harris, M. J. Moran, I. Aprahamian, *Proc. Natl. Acad. Sci. USA* **2018**, *115*, 9414–9422.
[13] Z. L. Pianowski, *Chem. Eur. J.* **2019**, *25*, 5128–5144.
[14] J. Volarić, W. Szymanski, N. A. Simeth, B. L. Feringa, *Chem. Soc. Rev.* **2021**, *50*, 12377–12449.
[15] R. D. Astumian, *Chem. Sci.* **2017**, *8*, 840–845.
[16] S. Kassem, T. van Leeuwen, A. S. Lubbe, M. R. Wilson, B. L. Feringa, D. A. Leigh, *Chem. Soc. Rev.* **2017**, *46*, 2592–2621.
[17] M. Baroncini, S. Silvi, A. Credi, *Chem. Rev.* **2020**, *120*, 200–268.
[18] D. R. S. Pooler, A. S. Lubbe, S. Crespi, B. L. Feringa, *Chem. Sci.* **2021**, *12*, 14964–14986.
[19] M. Kathan, S. Hecht, *Chem. Soc. Rev.* **2017**, *46*, 5536–5550.

[20] S. A. Endow, F. J. Kull, H. Liu, *J. Cell Sci.* **2010**, *123*, 3420–3424.
[21] C. B. Lindemann, K. A. Lesich, *J. Cell Sci.* **2010**, *123*, 519–528.
[22] A. Perrot, E. Moulin, N. Giuseppone, *Trends Chem.* **2021**, *3*, 926–942.
[23] Y. Qiu, Y. Feng, Q.-H. Guo, R. D. Astumian, J. F. Stoddart, *Chem* **2020**, *6*, 1952–1977.
[24] W.-Z. Wang, L.-B. Huang, S.-P. Zheng, E. Moulin, O. Gavat, M. Barboiu, N. Giuseppone, *J. Am. Chem. Soc.* **2021**, *143*, 15653–15660.
[25] C. Cheng, P. R. McGonigal, S. T. Schneebeli, H. Li, N. A. Vermeulen, C. Ke, J. F. Stoddart, *Nat. Nanotechnol.* **2015**, *10*, 547–553.
[26] G. Ragazzon, M. Baroncini, S. Silvi, M. Venturi, A. Credi, *Nat. Nanotechnol.* **2015**, *10*, 70–75.
[27] Y. Feng, M. Ovalle, J. S. W. Seale, C. K. Lee, D. J. Kim, R. D. Astumian, J. F. Stoddart, *J. Am. Chem. Soc.* **2021**, *143*, 5569–5591.
[28] T. Kudernac, N. Ruangsupapichat, M. Parschau, B. Macia, N. Katsonis, S. R. Harutyunyan, K.-H. Ernst, B. L. Feringa, *Nature* **2011**, *479*, 208–211.
[29] A. Saywell, A. Bakker, J. Mielke, T. Kumagai, M. Wolf, V. García-López, P.-T. Chiang, J. M. Tour, L. Grill, *ACS Nano* **2016**, *10*, 10945–10952.
[30] M. von Delius, E. M. Geertsema, D. A. Leigh, *Nat. Chem.* **2010**, *2*, 96–101.
[31] M. Škugor, J. Valero, K. Murayama, M. Centola, H. Asanuma, M. Famulok, *Angew. Chem. Int. Ed.* **2019**, *58*, 6948–6951; *Angew. Chem.* **2019**, *131*, 7022–7025.
[32] S. Chen, Y. Wang, T. Nie, C. Bao, C. Wang, T. Xu, Q. Lin, D.-H. Qu, X. Gong, Y. Yang, L. Zhu, H. Tian, *J. Am. Chem. Soc.* **2018**, *140*, 17992–17998.
[33] T. R. Kelly, H. De Silva, R. A. Silva, *Nature* **1999**, *401*, 150–152.
[34] R. Wilcken, M. Schildhauer, F. Rott, L. A. Huber, M. Guentner, S. Thumser, K. Hoffmann, S. Oesterling, R. de Vivie-Riedle, E. Riedle, H. Dube, *J. Am. Chem. Soc.* **2018**, *140*, 5311–5318.
[35] L. Greb, J.-M. Lehn, *J. Am. Chem. Soc.* **2014**, *136*, 13114–13117.
[36] L. Greb, A. Eichhöfer, J.-M. Lehn, *Angew. Chem. Int. Ed.* **2015**, *54*, 14345–14348; *Angew. Chem.* **2015**, *127*, 14553–14556.
[37] N. Koumura, R. W. J. Zijlstra, R. A. van Delden, N. Harada, B. L. Feringa, *Nature* **1999**, *401*, 152–155.
[38] M. M. Pollard, M. Klok, D. Pijper, B. L. Feringa, *Adv. Funct. Mater.* **2007**, *17*, 718–729.
[39] M. Klok, N. Boyle, M. T. Pryce, A. Meetsma, W. R. Browne, B. L. Feringa, *J. Am. Chem. Soc.* **2008**, *130*, 10484–10485.
[40] J. Chen, F. K.-C. Leung, M. C. A. Stuart, T. Kajitani, T. Fukushima, E. van der Giessen, B. L. Feringa, *Nat. Chem.* **2018**, *10*, 132–138.
[41] C. Gao, A. Vargas Jentzsch, E. Moulin, N. Giuseppone, *J. Am. Chem. Soc.* **2022**, *144*, 9845–9852.
[42] M. Kathan, S. Crespi, N. O. Thiel, D. L. Stares, D. Morsa, J. de Boer, G. Pacella, T. van den Enk, P. Kobauri, G. Portale, C. A. Schalley, B. L. Feringa, *Nat. Nanotechnol.* **2022**, *17*, 159–165.
[43] N. Koumura, E. M. Geertsema, A. Meetsma, B. L. Feringa, *J. Am. Chem. Soc.* **2000**, *122*, 12005–12006.
[44] D. Roke, S. J. Wezenberg, B. L. Feringa, *Proc. Natl. Acad. Sci. USA* **2018**, *115*, 9423–9431.
[45] Q. Li, G. Fuks, E. Moulin, M. Maaloum, M. Rawiso, I. Kulic, J. T. Foy, N. Giuseppone, *Nat. Nanotechnol.* **2015**, *10*, 161–165.
[46] J. T. Foy, Q. Li, A. Goujon, J.-R. Colard-Itté, G. Fuks, E. Moulin, O. Schiffmann, D. Dattler, D. P. Funeriu, N. Giuseppone, *Nat. Nanotechnol.* **2017**, *12*, 540–545.
[47] F. K.-C. Leung, T. van den Enk, T. Kajitani, J. Chen, M. C. A. Stuart, J. Kuipers, T. Fukushima, B. L. Feringa, *J. Am. Chem. Soc.* **2018**, *140*, 17724–17733.
[48] L. Ribovski, Q. Zhou, J. Chen, B. L. Feringa, P. van Rijn, I. S. Zuhorn, *Chem. Commun.* **2020**, *56*, 8774–8777.
[49] J. Hou, A. Mondal, G. Long, L. Haan, W. Zhao, G. Zhou, D. Liu, D. J. Broer, J. Chen, B. L. Feringa, *Angew. Chem. Int. Ed.* **2021**, *60*, 8251–8257; *Angew. Chem.* **2021**, *133*, 8332–8338.
[50] A. Ryabchun, F. Lancia, J. Chen, D. Morozov, B. L. Feringa, N. Katsonis, *Adv. Mater.* **2020**, *32*, 2004420.
[51] J. Hou, G. Long, W. Zhao, G. Zhou, D. Liu, D. J. Broer, B. L. Feringa, J. Chen, *J. Am. Chem. Soc.* **2022**, *144*, 6851–6860.
[52] C. Poloni, M. C. A. Stuart, P. van der Meulen, W. Szymanski, B. L. Feringa, *Chem. Sci.* **2015**, *6*, 7311–7318.
[53] D. J. van Dijken, J. Chen, M. C. A. Stuart, L. Hou, B. L. Feringa, *J. Am. Chem. Soc.* **2016**, *138*, 660–669.
[54] J.-R. Colard-Itté, Q. Li, D. Collin, G. Mariani, G. Fuks, E. Moulin, E. Buhler, N. Giuseppone, *Nanoscale* **2019**, *11*, 5197–5202.
[55] G. Mariani, J.-R. Colard-Itté, E. Moulin, N. Giuseppone, E. Buhler, *Soft Matter* **2020**, *16*, 4008–4023.
[56] Q. Li, J. T. Foy, J.-R. Colard-Itté, A. Goujon, D. Dattler, G. Fuks, E. Moulin, N. Giuseppone, *Tetrahedron* **2017**, *73*, 4874–4882.
[57] A. Perrot, E. Buhler, D. Dattler, N. Giuseppone, E. Moulin, S. Prevost, **2021**, https://dx.doi.org/10.5291/ILL-DATA.9-11-2004.
[58] M. Klok, W. R. Browne, B. L. Feringa, *Phys. Chem. Chem. Phys.* **2009**, *11*, 9124–9131.
[59] S. Saeki, N. Kuwahara, M. Nakata, M. Kaneko, *Polymer* **1976**, *17*, 685–689.
[60] Y. C. Bae, S. M. Lambert, D. S. Soane, J. M. Prausnitz, *Macromolecules* **1991**, *24*, 4403–4407.

Manuscript received: January 6, 2023
Accepted manuscript online: January 30, 2023
Version of record online: ■■, ■■

Research Articles

Hydrogels

A. Perrot, W.-z. Wang, E. Buhler, E. Moulin, N. Giuseppone* ——— **e202300263**

Bending Actuation of Hydrogels through Rotation of Light-Driven Molecular Motors

The integration of light-driven rotary motors in polymer networks leads to active hydrogels that can be engineered as macroscopic bending actuators. In this configuration, lifting experiments reveal that a single molecular motor can pick up loads of 200 times its own molecular weight.